

## 4 Production and Spectroscopy of Antihydrogen

C. Amsler, A. Glauser, D. Grögler, O. Iannarelli, D. Lindelöf,  
N. Madsen, H.P. Meyer, H. Pruyss, and C. Regenfus

*collaboration with:*

CERN, MIT, Universities of Aarhus, Brescia, Genoa, Pavia, Rio de Janeiro, Tokyo, Wales

(ATHENA/AD-1 Collaboration).

### 4.1 Introduction

The physics goal of the ATHENA experiment [1] is a direct comparison of the properties of antihydrogen and hydrogen atoms (for a recent review, see Ref.[2]). The final target is the most precise test of CPT invariance in the lepton and baryon sector. The long lifetime (122 ms) of the metastable (anti-)hydrogen 2S level is associated with a relative natural line width of  $5 \times 10^{-16}$  for the 1S-2S transition, which can be exploited by two-photon laser spectroscopy. In addition, such high precision measurements would give valuable experimental information on the gravitational interaction of antihydrogen, because a change in the 1S-2S transition frequency could also originate from a different redshift of antihydrogen and hydrogen atoms in the gravitational field of the earth. So far, only the existence of antihydrogen was demonstrated experimentally with the production of a few dozens of energetic antihydrogen atoms at LEAR [3] and at FNAL [4].

The current phase 1 of ATHENA is devoted to the formation of large quantities of antihydrogen atoms in Penning traps, with the goal of obtaining large rates ( $> 1$  Hz) at the lowest possible kinetic energy ( $\ll 1$  eV). The formation rate depends on the densities of antiproton and positron plasmas, the absolute number of particles, their temperature, and on the trap potentials. The result of these studies will determine the apparatus of phase 2, the laser spectroscopic precision measurements.

The ATHENA apparatus was installed and commissioned in 1999/2000 at one of the three extraction lines of the new Antiproton Decelerator (AD) at CERN. The AD captures  $5 \times 10^7$  antiprotons at 3.5 GeV/c and decelerates them to 100 MeV/c (5.3 MeV kinetic energy), using stochastic and electron cooling, before extracting the antiproton bunch within 250 ns. Steady improvements by the AD team resulted in an intensity of  $3\text{--}4 \times 10^7$  antiprotons per spill, with a cycle time of 96 seconds. The number of antiprotons per bunch is now exceeding the value given in the design report.

### 4.2 Experimental setup

The apparatus (Fig.4.1) consists of (i) an antiproton capture trap and a recombination trap, located in a cryogenic vacuum enclosure inside a large bore 3 T solenoid, (ii) a positron accumulator for collecting, cooling and transferring a large number of positrons ( $> 10^8$ ) every 3–5 minutes to the recombination trap, and (iii) a high granularity large solid angle antihydrogen detector. More details on the apparatus are given in previous annual reports.

The incoming antiproton pulse is monitored by a  $67 \mu\text{m}$  thin segmented silicon beam counter. The range of antiprotons with kinetic energy of 5.3 MeV is only about  $200 \mu\text{m}$  in silicon. The amount of material in the beam was carefully optimised to obtain the maximum number of captured antiprotons by introducing a foil with variable tilt angle. The optimum thickness was determined by trapping antiprotons, releasing them after a delay of several

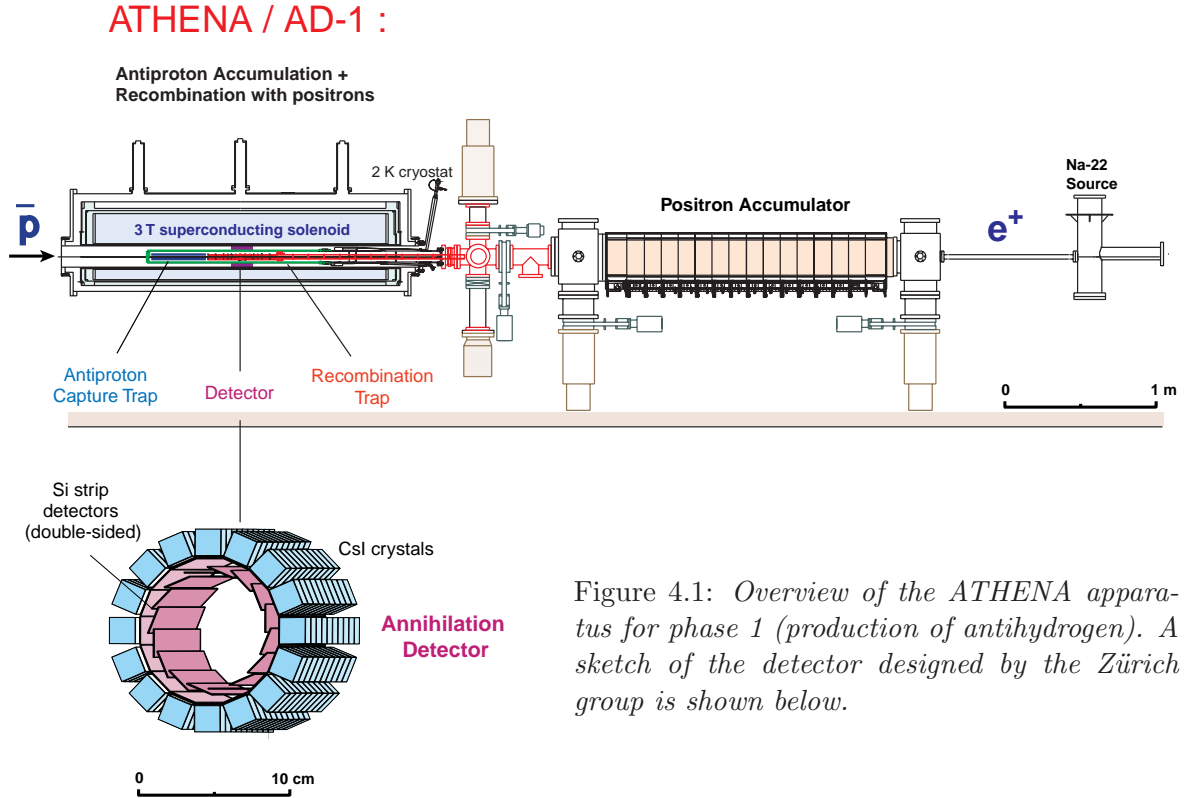


Figure 4.1: Overview of the ATHENA apparatus for phase 1 (production of antihydrogen). A sketch of the detector designed by the Zürich group is shown below.

seconds and measuring the number of annihilations. After determination of the optimal value, the tilted foil was removed and  $44 \mu\text{m}$  of aluminium was added to the degrader material at the trap entrance.

The antiproton catching trap consists of cylindrical electrodes of various lengths and radii  $1.25 \text{ cm}$  made of gold-plated aluminium. Seven electrodes are used to create a harmonic field region in the capture region, three upstream and downstream to shape the electric field during various phases of particle transfer and handling, and two at the ends for applying the high voltage necessary to capture antiprotons. The exit electrode is biased to  $-10 \text{ kV}$ . The entrance electrode (HVL) is quickly lowered to  $-10 \text{ kV}$ , triggered by the signal from an external scintillator monitoring the arrival of antiprotons. We are able to capture about  $20'000$  antiprotons from a single AD shot of a few  $10^7$  antiprotons.

Before antiproton injection, a few  $10^8$  electrons are loaded from an electron source (heated filament). The electron cloud quickly cools down to ambient cryogenic temperature ( $10 \text{ K}$ ) by emitting synchrotron radiation. Antiprotons with energies in the keV range are then cooled within  $20\text{-}30 \text{ s}$  by interactions with the cold electrons stored in the central part of the catching trap. The lifetime of cooled antiprotons was measured to exceed ten hours. The high voltage electrodes could then be lowered to capture further  $\bar{p}$  and several AD shots were successfully stacked.

Positrons are emitted from a  $50 \text{ mCi } ^{22}\text{Na}$  source. After moderation in solid neon the low energy beam of  $7 \times 10^6$  positrons/s is guided into a  $0.14 \text{ T}$  magnetic field. The positrons enter an array of cylindrical electrodes, which have increasing radii and are biased at appropriate electric potentials. They are moderated by inelastic collisions with a nitrogen buffer gas. The size and radial position of the plasma is measured by dumping the positrons on a movable, segmented Faraday cup detector. One of the trapping electrodes is split into six azimuthal segments to compress the plasma by applying a rotating electric field of several hundred

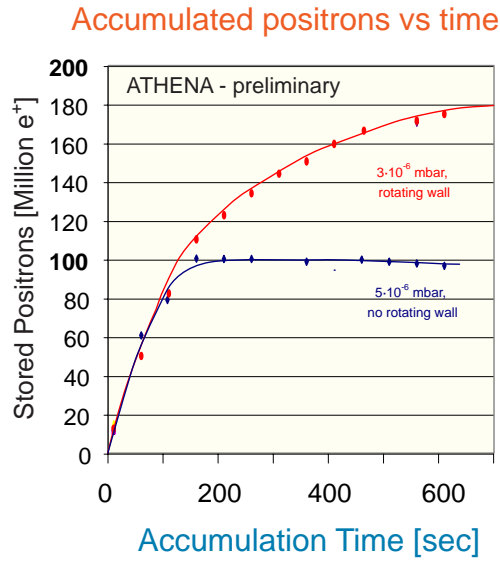


Figure 4.2: Number of trapped positrons as a function of time, with and without rotating wall compression.

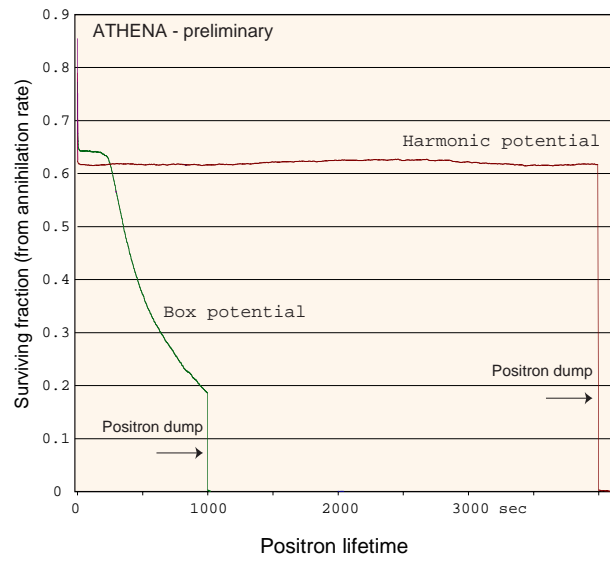


Figure 4.3: Positron lifetime in the recombination trap, using a box potential or a harmonic trap potential.

kHz (“rotating wall”). During compression the plasma is cooled by the nitrogen buffer gas. The rotating wall technique reduces the diameter of the positron plasma from 15 to 4 mm. Figure 4.2 shows the number of positrons accumulated as a function of time:  $1.7 \times 10^8$  positrons were accumulated in 450 seconds while without compression this number drops to about  $10^8$ .

Positrons are transferred into the recombination trap by extracting the positron cloud from the accumulator trap: the buffer gas is pumped out and a magnet is turned on (1.2 T in 20 ms). The electrostatic trap is opened and the transfer electrodes are biased to accelerate the positrons towards the recombination trap. The transfer efficiency is measured by shooting the positrons directly on a Faraday cup and by measuring the annihilation signal with a CsI detector. Positrons are routinely transferred with efficiencies exceeding 50 %. The positrons are captured within 1 s in the recombination region, where they cool by synchrotron radiation to the ambient temperature (10 K). Positron lifetimes of several hours have been achieved with a harmonic trap potential (Fig.4.3) and about 25 million trapped and cooled positrons were observed.

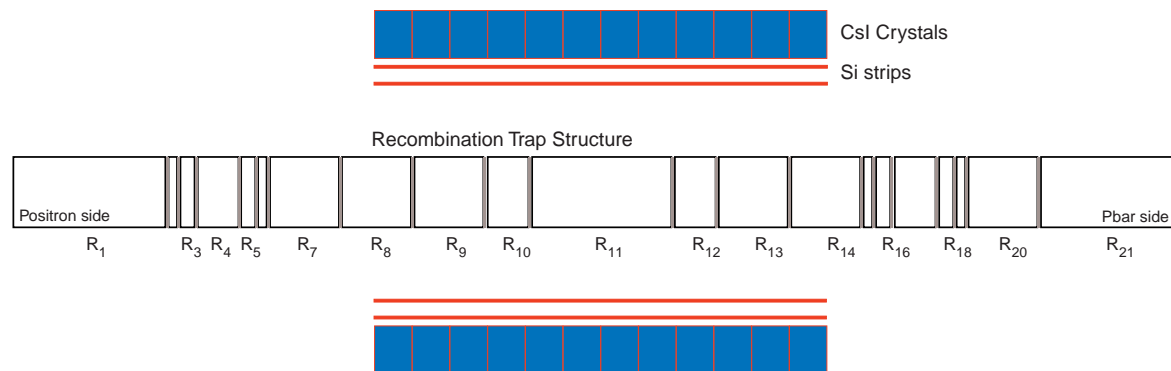


Figure 4.4: Side view of the recombination trap and the antihydrogen detector.

The recombination trap (Fig.4.4) consists of 21 cylindrical electrodes with radii 1.25 cm and a total length of 41 cm. With this complicated structure we will be able to cool and compress the positron cloud with the rotating wall technique, store the antiprotons transferred from the capture trap, overlap the antiproton and positron clouds, and monitor the plasma parameters (density, temperature).

The antihydrogen detector built by the Zürich group is now commissioned and is being used to detect antiproton and positron annihilations with the rest gas or the trap electrodes and to measure the position, size and shape of the plasma. The compact and highly granular detector observes the annihilation products of antiproton and positron annihilations. Since antihydrogen atoms are not confined by the electromagnetic fields of the recombination trap, they propagate freely and annihilate at the electrode surfaces within 1 ms. To maximise the detection efficiency, the detector is installed as close as possible to the recombination trap, inside the vacuum bore of the superconducting solenoid and around the cold nose containing the recombination trap system. Antiproton annihilation produces on average three charged pions and three high energy  $\gamma$ 's while positron annihilation produces two 511 keV back-to-back photons (Fig.4.5). The charged pions are detected in two cylindrical layers of 16 double-sided silicon microstrip detectors (8192 channels) at average radii of 3.9 cm and 4.5 cm, respectively. The 511 keV photons from positron annihilation are detected by 16 rows of 12 pure CsI crystals ( $13 \times 17.5 \times 17 \text{ mm}^3$ ) read out by photodiodes. Figure 4.6 shows a photograph of the detector assembly. Details can be found in previous annual reports, diploma works [5] and in Ref.[6].

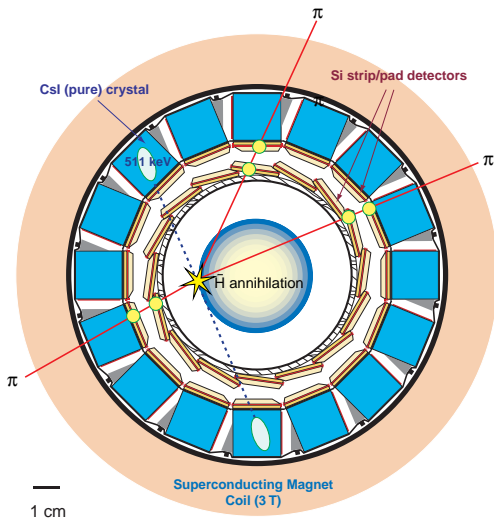


Figure 4.5: *Antihydrogen annihilation detector.*

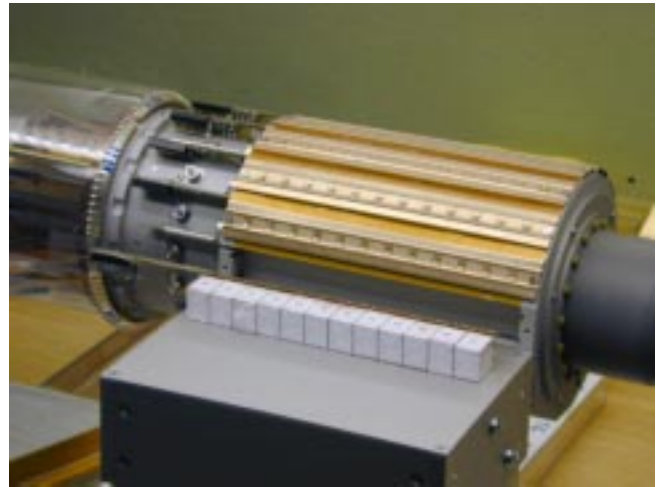


Figure 4.6: *Antihydrogen detector during assembly showing a row of crystals.*

A high granularity of the detector and good resolution on the photon energies are required by background considerations: antiproton annihilating on the electrode surface can fake antihydrogen annihilation, since high energy photons from the annihilation convert e.g. in the magnet coil, creating positrons which annihilate outside the detector region. This background can be suppressed by requiring the two back-to-back 511 keV photons to emerge from the annihilation vertex. The latter is determined from the tracks of the emitted pions and is required to lie at the electrode radius. The resolution on the annihilation vertex is 3 mm (r.m.s).

The detector located inside the cold bore of the magnet is operated at a temperature

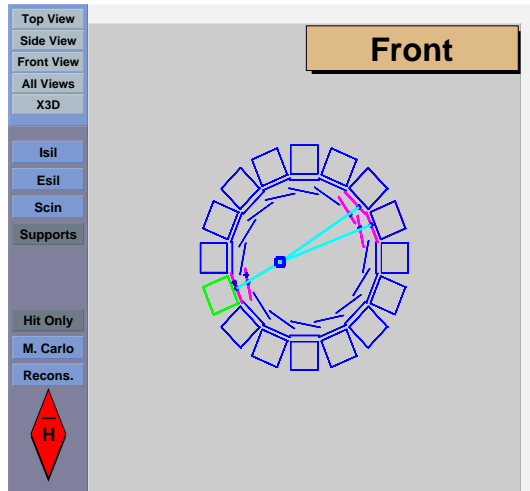


Figure 4.7: *Event display of a 3-prong annihilation event from a trapped antiproton hitting the cylindrical electrode. The hits in the strip detectors and the associated crystals are visible.*

between 77 and 140 K. The performance of pure CsI crystals and photodiodes (light yield and efficiency) were measured at low temperature: the photon yield at 80 K is on average, 30'000 per MeV, as compared to 3'200 per MeV at room temperature. A record value of 50'000 per MeV was reported [6]. The first annihilations from antiprotons in the recombination trap were observed during summer 2001. Figure 4.7 shows a 3-prong annihilation event from a trapped antiproton.

The capability to measure the vertex of antiproton annihilations with rest gas atoms or on trap electrodes is a new tool for (destructive) plasma diagnostics. We can monitor the shape of the antiproton cloud and follow its evolution in time. Figure 4.8 shows the  $\bar{p}$  annihilation vertex distribution in the recombination trap in three projections. Annihilations on a trap electrode at a radius of 1.25 cm are visible. Annihilations at smaller radii are due to collisions with rest gas atoms. The resolution of  $\sigma = 3\text{--}4$  mm stems from the unknown track curvatures in the magnetic field (which cannot be measured with two layers of strip detectors) and is fully compatible with expectations.

The transfer, capture and storage of positrons in the recombination trap can be monitored by measuring their annihilations with our CsI crystals. The annihilation signal from one of the 192 crystals is shown in Fig.4.9 and the energy distribution of the 511 keV  $\gamma$ 's in Fig.4.10.

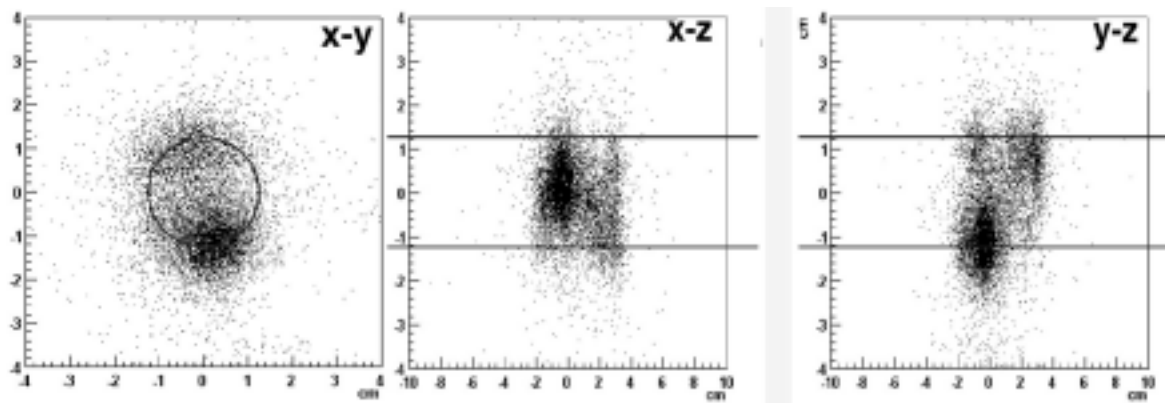


Figure 4.8: *Distribution of the antiproton annihilation vertices in the three projections; the  $z$  direction is the along the symmetry axis of the cylindrical trap. The lines show the boundary (wall) of the trap.*

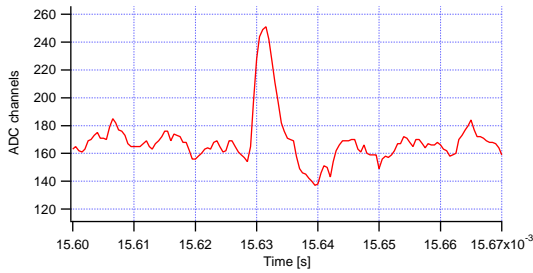


Figure 4.9: *Time signal from a 511 keV photon observed in one of the 192 CsI crystals of the antihydrogen detector surrounding the recombination trap filled with positrons at a temperature of 140 K.*

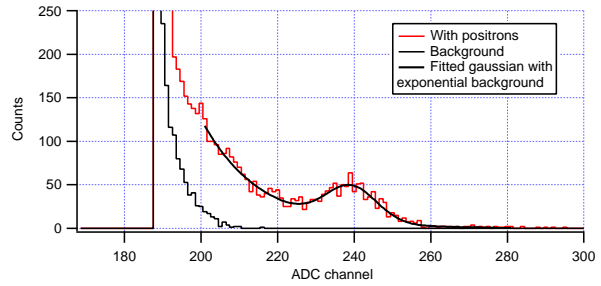


Figure 4.10:  *$\gamma$ -Energy distribution from a CsI crystal when the trap is filled with positrons. Top: spectrum from  $e^+e^-$  annihilation, with a clear peak at 511 keV, and a shoulder due to Compton scattered gammas. Bottom: background spectrum.*

The background spectrum is clearly separated from the 511 keV peak and its associated Compton edge.

### 4.3 Avalanche photodiodes

To reduce costs and also to match the surface of our crystals the photodiodes were manufactured from the same wafers as the silicon strip detectors, with very thin entrance windows to maximise the efficiency for detection of blue light from CsI. However, we discovered during the 2001 runs that the electronic noise from many of the SINTEF photodiodes had increased substantially, reaching unacceptable levels (signal over noise ratio of 5 or less) so that 511 keV photons could not be detected with the good resolution (better than 10% [6]) achieved previously. The problem was traced to oxidation of the electrical contacts to the photodiode (possibly due to the iodine of CsI). Commercially available Hamamatsu pin-photodiodes were found to yield insufficient electron/hole pairs, essentially due to their small size.

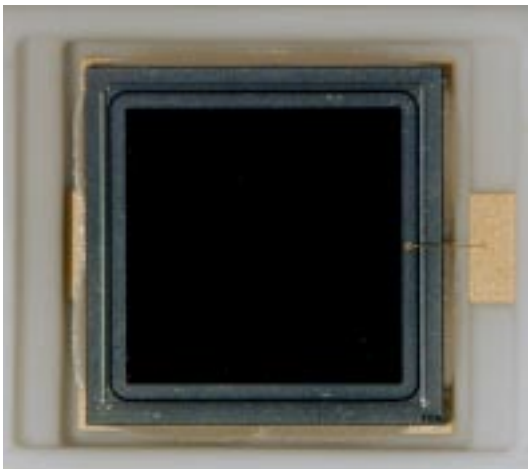


Figure 4.11: *Avalanche photodiode ( $5 \times 5 \text{ mm}^2$ ) used for the CMS experiment with its epoxy window removed.*

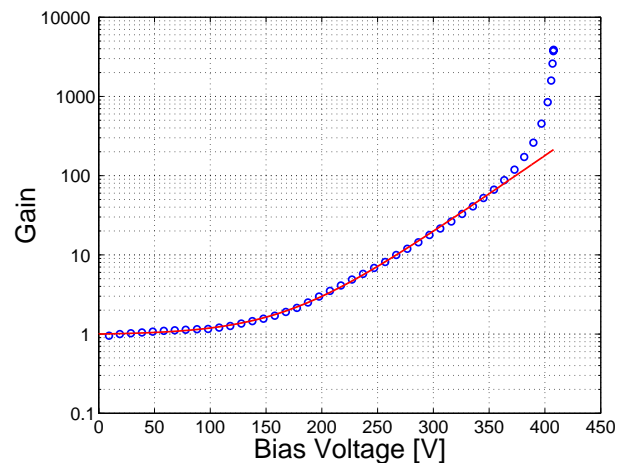


Figure 4.12: *Gain of an avalanche photodiode at room temperature as a function of bias voltage  $V$ . The curve is a fit with a function of the form  $a + b \exp(cV)$ .*

As an alternative solution we tried avalanche photodiodes (APD) which have the advantage of a large gain and hence a much better signal-over-noise ratio. Encouraging tests were performed with spare APD's obtained from the CMS experiment not satisfying their stringent gain requirements. However, we first had to remove the epoxy windows which break at liquid nitrogen temperature. The best stripping agent was found to be sulfuric acid. Figure 4.11 shows a photograph of one of the 300 APD's purchased from CMS (a small batch from their 160'000 supply!). The gain of the APD as a function of bias voltage was measured with a pulsed (blue) light emitting photodiode (Fig.4.12). The plateau at low voltage corresponds to unit gain, the rise is due to the generated avalanche in the diode. The voltage at which multiplication starts depends on temperature. The advantage of APD's for ATHENA is the very low dark current at low temperature, so that the signal can be amplified to very high values (with a gain of  $10^4$  a signal-over-noise ratio of the same order of magnitude can be reached for 511 keV photons!). The useful gain is however limited by our VA2 preamplifiers. We settled for a gain of 20 (compared to 50 for CMS) corresponding to a signal-over-noise ratio of about 100.

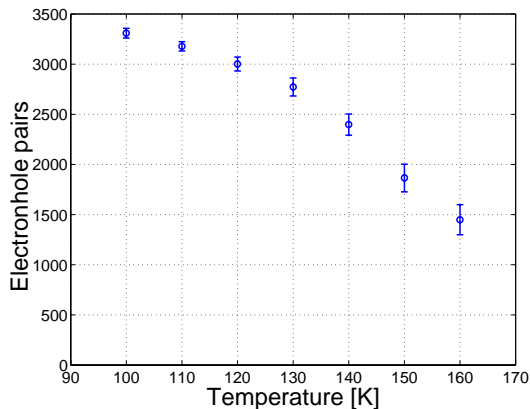


Figure 4.13: Number of primary electron-hole pairs in the APD per 1 MeV energy loss in CsI, as a function of temperature.

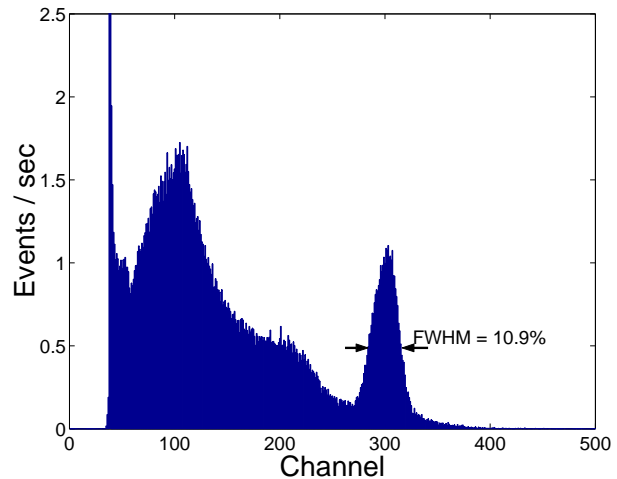


Figure 4.14:  $^{137}\text{CsI}$  spectrum from a CsI crystal coupled to an APD measured at liquid nitrogen temperature. The 662 keV photopeak has a resolution of 10.9 % (FWHM) and the Compton shoulder is clearly visible.

Figure 4.13 shows the number of electron-hole pairs produced for an energy loss of 1 MeV in the CsI crystals. The typical yield of about 3'000/MeV is much lower than our 30'000 with SINTEF diodes [6]. This is due to the much smaller size of the APD's ( $5 \times 5 \text{ mm}^2$  compared to  $17 \times 13 \text{ mm}^2$ ) and also to the thin air gap between the diode and the crystal. However, the energy resolution is now determined by the light collection efficiency while noise becomes negligible. The resolution is not significantly worse than that obtained with SINTEF diodes (Fig.4.14).

We also found that APD's were much more sensitive to the blue component of light than to the red one. Therefore the red dye used previously as wavelength shifter to coat the crystals was removed and all SINTEF diodes replaced by APD's for the forthcoming 2002 runs.

#### 4.4 Summary and outlook

To summarise, in 2001 ATHENA demonstrated the trapping, cooling and transfer to the recombination trap of  $2 \times 10^4$  antiprotons. Several antiproton shots were stacked in the antiproton capture trap where a lifetime of 10 hours was measured. This allows us to reach the target of  $10^5$  stored and cooled antiprotons. In the positron accumulator we accumulated  $1.5 \times 10^8$  positrons in five minutes which corresponds to an increase by two orders of magnitude with respect to the previous year. The transfer of  $10^8$  positrons from the accumulator to the recombination trap was demonstrated. Trapping and cooling led to  $2.5 \times 10^7$  positrons with a lifetime of several hours. The target of  $10^8$  stored and cooled positrons is thus within reach.

The main goal for the coming year is to store simultaneously  $10^5$  antiprotons and  $10^8$  positrons in the recombination trap. We will search for annihilation of antihydrogen atoms hitting the electrodes using the antihydrogen detector. We will drive the antiprotons through the positron plasma with a frequency which maximises the spontaneous antihydrogen formation rate while keeping the positron temperature as low as possible. Once the production of antihydrogen has been demonstrated we will measure its production rate as a function of plasma density and temperature, number of particles and trap potentials. Based on the  $\bar{p}$  and  $e^+$  intensities given above and on theoretical models of spontaneous radiative recombination, we expect the production of about 0.1 to 1 antihydrogen atom per second. Depending on the yield of anti-atoms with very low kinetic energy ( $< 0.05$  meV), the optimal setup for a 1S-2S precision experiment will be designed. Meanwhile the Zürich group is involved in the preparation of the laser system, in particular the frequency doubler to produce the 243 nm light inducing the 1S to 2S transition by recoilless two-photon absorption. The year 2002 promises to be very exciting.

## References

- [1] ATHENA proposal, M.H. Holzschneider *et al.*, CERN-SPSLC/P302, October 1996, see also <http://www.cern.ch/athena/>.
- [2] M. H. Holzschneider and M. Charlton, Rep. Prog. Phys. 62, 1 (1999); see also C. Amsler *et al.*, *Antihydrogen Production and Precision Spectroscopy with ATHENA*, in “The Hydrogen Atom, Precision Physics of Simple Atomic Systems”, edited by S.G. Karshenboim *et al.*, Springer Lecture Notes in Physics, Berlin, 2001, p. 469-488.
- [3] G. Baur *et al.*, Phys. Lett. B368 (1996) 251.
- [4] G. Blanford *et al.*, Phys. Rev. Lett. 80 (1998) 3037.
- [5] P. Niederberger, *Untersuchung von CsI-Szintillatoren bei tiefen Temperaturen*, Universität Zürich, 1999;  
R. Brunner, *Aufbau und Test eines Microstrip-Detektors für das ATHENA-Experiment*, Universität Zürich, 2000;  
D. Grögler, *Temperature Dependence of Pure CsI between 77 K and 165 K and the Performance of Wavelength Shifters*, Universität Zürich, 2000.
- [6] C. Amsler *et al.*, N.I.M. A 480 (2002) 492.